Journal of the Physical Society of Japan
Vol. 63, No. 12, December, 1994, pp. 4573–4582

Ferromagnetic Transition of Heisenberg Ferromagnetic Metal of CoS_2 —Static Critical Properties—

Haruhiro HIRAKA and Yasuo ENDOH

Department of Physics, Tohoku University, Aramaki Aza Aoba, Aoba-ku, Sendai 980-77

(Received July 4, 1994)

The static magnetic properties near the Curie temperature in CoS_2 have been thoroughly studied by using various experimental techniques from high quality single crystals, which were grown by the chemical transport technique. A very small anisotropy in magnetization confirms that CoS_2 is the best system to apply the Heisenberg Hamiltonian. The critical indices obey the static scaling hypothesis, which indicates negligible effect of the temperature-induced local moment on the ferromagnetic transition. However, the static critical properties suggest that the magnetic transition is close to the tricritical point, although the magnetic transition in CoS_2 is continuous.

[single crystal CoS_2, critical indices, scaling law, tricritical point, critical neutron scattering]

§1. Introduction

CoS_2 of the pyrite structure is a metallic ferromagnet whose Curie temperature, T_c is about 120 K. The atomic moment is 0.84 μ_B per Co atom.[1,2] The Co atoms form a face-centered cubic (fcc) structure and sit on the center of the sulfur octahedron. The strong cubic crystalline field splits d-bands to the lower t_{2g} and upper e_g, and the Fermi level lies in the middle of the upper e_g band. Due to the fact of the cubic structure and the nearly half filled band, the magnetic Hamiltonian must be isotropic. Indeed the anisotropy of the magnetic properties is quite small.[3,4] Therefore one can imagine that the experimental results of the magnetic properties can well be fitted to the simple model Hamiltonian, which is not true.

The magnetic susceptibility of CoS_2 in the paramagnetic region is temperature dependent but the linearity of χ^{-1} in temperature breaks at around 350 K above which the effective moment seems to saturate at 1 μ_B.[2] Moriya interpreted this anomalous thermal behavior in the context of the self-consistent renormalization (SCR) theory that the local magnetic moment does change thermally by the effect of the renormalized spin fluctuations.[5] The major interest in the present study on the spin correlations in CoS_2 is whether the effect of the renormalized spin fluctuations influences the critical behavior near T_c. The anomalous behavior of the specific heat near the Curie temperature was the issue whether the result is comprehensible in the context of the SCR theory. The SCR theory claims that the critical divergence for the weak itinerant ferromagnets must be suppressed from the mean field value in the specific heat in particular due to the effect of mode-mode coupling between the low energy spin fluctuations.[6] The mean field theory for the Heisenberg ferromagnet predicts the logarithmic divergence of the specific heat; the critical index α should be 0. On the other hand the real experimental value of α ($T > T_c$) or α' ($T < T_c$) reported for CoS_2 was 0.3 or 0.8.[7]

In this respect, we are very much interested in the fact that the rapid change in the magnetic properties when Se is substituted to S in CoS_2. T_c drops substantially through the substitution and vanishes at $Co(Se_{0.11}S_{0.89})_2$.[2] Another characteristic feature in the mixed system of $Co(Se_xS_{1-x})_2$ is the fact that the ferromagnetic transition seems to be discontinuous.[8] It is well established that the thermal be-

havior at the tricritical point quite differs from that of the second order phase change and also the critical indices of the second order transition are largely influenced when the second order critical line approaches to the tricritical point.[9] Therefore it is very important at this status that thermal behavior must be reexamined by using the high quality single crystal. Then we will test all the critical indices again whether they fill the scaling hypothesis, since the scaling hypothesis is set up in the system that well defined saturated magnetic moments interact with each other, which is treated by the model Hamiltonian.

We do expect the different dynamical behavior of the critical scattering spectra, if the local induced moment plays a dominant role by the effect of the renormalized spin fluctuatiuons as claimed by the SCR theory. However we don't know the scaling hypothesis can be satisfied without any condition. Prior to the dynamical studies, we have performed all the static measurements near T_c and tested the scaling hypothesis from the high quality single crystals which were prepared by the technique of the chemical transport.[10]

The format of the paper is the following. The experiments will be described by the sample preparation followed by the experimental procedure and results, magnetization, specific heat and neutron scattering. The §4 is devoted to the discussion of the present results with the concluding remarks.

§2. Sample Preparation[10]

Polycrystals of CoS_2 were made of cobalt (99.9%) and sulfur (99.999%) raw material powder. The nominal mixtures of CoS were sealed in silica tubes under the pressure of 10^{-2} torr and then the mixtures were kept at 700°C for 3 days. After quenched into water they were ground and other powder of sulfur was added so as to be the nominal mixtures of CoS_2. The materials were sealed again with excess sulfur and reacted for 7 days under the same condition. The X-ray powder diffraction revealed that the specimen contains only a single phase of pyrite structure.

We grew single crystals by the method of chemical vapour deposition, which we describe here in detail. The grown condition is rather difficult to be determined but the following condition was found to be appropriate. Silica tubes of 1 cm diameter and about 15 cm long were used. The powder of CoS_2 with the weight of $0.5 \sim 1$ g was sealed into the tubes with 0.4 atm of Cl_2 gas. We have found a proper condition to grow a reasonable size of the crystal; 780°C at the hot zone and 720°C at the cool zone, growing period is about 2 weeks. The single crystals show metallic lustre and often exhibited high symmetric cleavage surfaces. The typical mosaicness of $0.30° \sim 0.35°$ is determined by a locking curve from neutron scattering.

§3. Experimental Procedures Near T_c and Results

3.1 Magnetic anisotropy

The magnetic anisotropy of CoS_2 has been measured preliminarily by using a conventional vibrating sample magnetometer (VSM). The sample used here was shaped into a sphere with the diameter of 2.7 mm. We measured the *M-H* curves along the [111] and [100] crystal directions at both 4.2 K and 77.4 K. The *M-H* curves were corrected by taking into account the observed demagnetization factor (0.335), and the corrected data are shown in Fig. 1. The easy axis in magnetization is [111] and magnetic anisotropy was found to be very small, which is represented by the cubic anisotropy constants K_1 of -1.7×10^{-4} and -0.3×10^{-4} erg cc^{-1} at 4.2 K and 77.4 K, respectively. This result coincides with those obtained from torque measurements[3] and FMR experiments.[4]

3.2 Magnetization measurements

The isothermal magnetization curves were obtained in the vicinity of T_c by using the VSM. A single crystal was shaped into a sphere with the diameter of 3.5 mm. Due to the small magnetic anisotropy, we decided that it is not necessary to measure at a fixed crystal axis. A calibrated chromel-constantan thermocouple (CRC) was attached on the sample as the thermometer. The isothermal magnetization was measured near T_c in varying the magnetic field up to 12 kOe. The temperature stability during one scan was $\Delta T \leq \pm 0.03$ K.

Magnetization M at T_c, spontaneous mag-

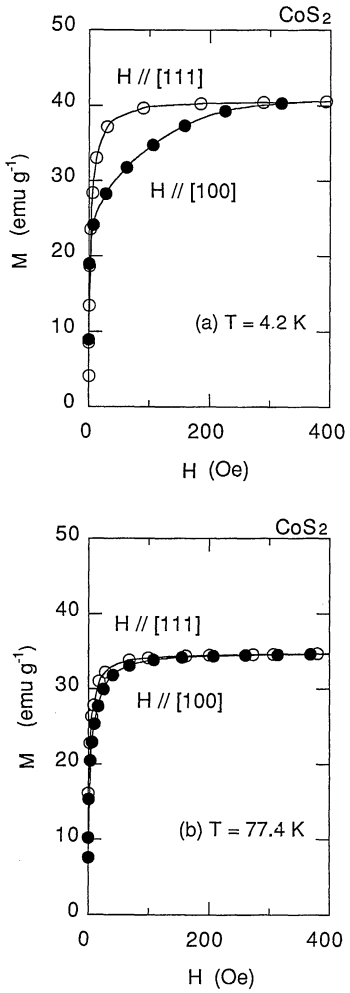

Fig. 1. Field dependence of magnetization of a single crystal CoS_2 in [111] and [100] crystal axes at (a) 4.2 K and (b) 77.4 K.

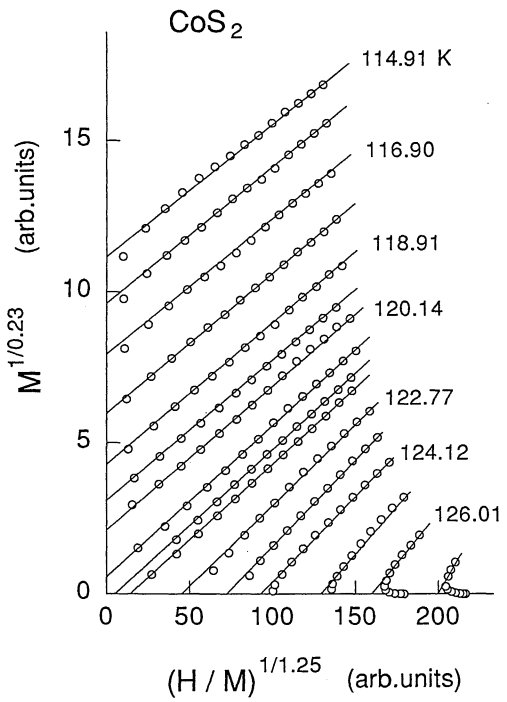

Fig. 2. A plot of isothermal magnetization data using eq. (4) with $\beta=0.23$ and $\gamma=1.25$.

netization M_s and zero field susceptibility χ_0 near T_c obey power laws:[11]

$$M_s \propto (T_c - T)^{\beta} \quad T < T_c, \tag{1}$$

$$\chi_0 \propto (T - T_c)^{-\gamma} \quad T > T_c, \tag{2}$$

$$M \propto H^{1/\delta} \quad T = T_c. \tag{3}$$

We analyzed the data of the isothermal magneatization with the expression proposed by Arrot and Noakes:[12]

$$c_1(H/M)^{1/\gamma} = \varepsilon_c + c_2 M^{1/\beta};\ \varepsilon_c \equiv \frac{T - T_c}{T_c} \tag{4}$$

where both c_1 and c_2 are numerical constants and H, the effective magnetic field. The linear relation between $M^{1/\beta}$ and $(H/M)^{1/\gamma}$ holds for CoS_2 as is shown in Fig. 2, from which M_s and χ_0 are deduced through extrapolations to the ordinate and abscissa respectively. Three critical indices as well as T_c were determined by this analysis over the reduced temperature range of $2\times10^{-3} < |\varepsilon_c| < 6\times10^{-2}$; $\beta = 0.23\pm0.02$, $\gamma = 1.25\pm0.05$, $\delta = 6.4\pm0.2$ and $T_c = 121.13\pm0.04$ K.

3.3 *Specific heat measurements*

The zero field specific heat of CoS_2 has been measured near T_c by using an ac calorimetric technique. A single crystal shaped into a disk with the diameter of 2 mm and the thickness 0.2 mm was used for the present experiments. The temperature was monitored with a calibrated CRC thermocouple junction attached on a surface of the specimen, while an opposite surface was heated up periodically by a heat pulse of a halogen light source. Data were taken continuously as the temperature was increased.

A preliminary measurement was done over the temperature region from 10 K to 200 K.

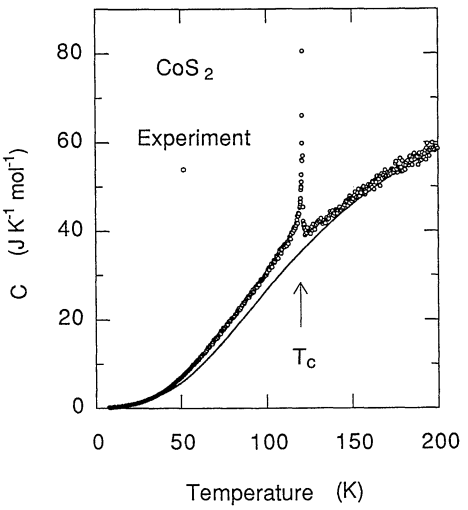

Fig. 3. Specific heat of a single crystal CoS_2 as a function of temperature. The solid curve is computed for lattice and electron contributions using $3C_D(\theta_D/T)+\gamma T$, where C_D, θ_D and γ are Debye specific heat function, Debye temperature and coefficient of electronic specific heat, respectively; $\theta_D=542$ K and $\gamma=25.8$ mJ K^{-2} mol^{-1}.

The experimental result is presented in Fig. 3, in which our data were normalized to absolute values at $T=200$ K utilizing the data of Ogawa and Yamadaya.[7] The contribution from the lattice and electronic terms was derived from the data taken at a low tempetrature side with $\theta_D=542$ K and $\gamma=25.8$ mJ K^{-2} mol^{-1}, where θ_D and γ are the Debye temperature and the coefficient of electronic specific heat respectively. The reasonable agreement between the experiment and calculation using these two parameters is seen at both ends higher or sufficiently lower than T_c. In order to deduce the magnetic part of specific heat, we fixed such a solid curve in Fig. 3 that is assumed to be the background for magnetic specific heat in the following analysis.

We ran the specific heat measurements three times near T_c and separated the magnetic contribution, C_{mag}, using above mentioned correction of both electronic and lattice parts. Then, the results were analyzed with the following asymptotic form;

$$C_{mag}=A^+\varepsilon_c^{-\alpha}+B^+ \quad (T>T_c) \quad (5)$$

$$=A^-|\varepsilon_c|^{-\alpha'}+B^- \quad (T<T_c). \quad (6)$$

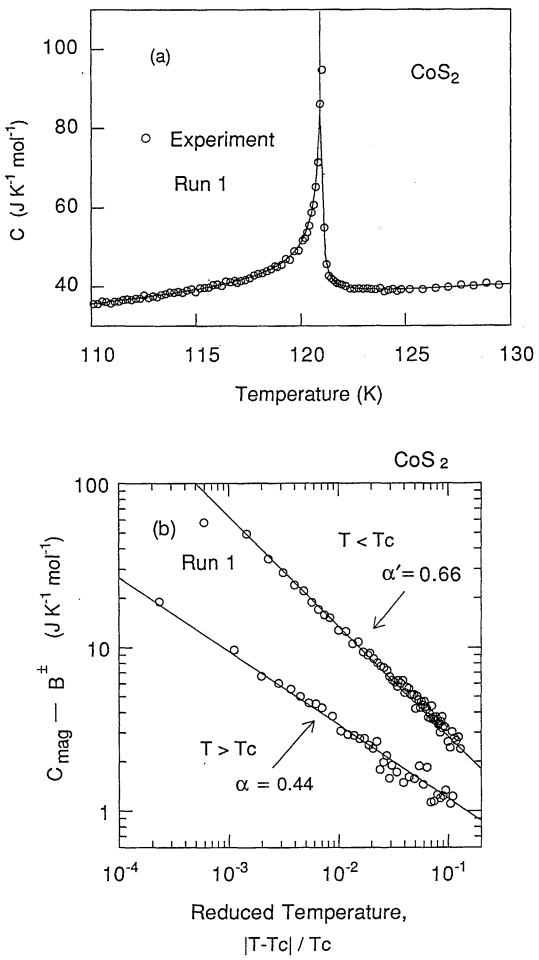

Fig. 4. (a) Specific heat of a single crystal CoS_2 near T_c. The smooth curves are drawn through eq. (5) and (6), using seven parameters obtained from least-square fits. (b) A conventional replot of the specific heat as a function of reduced temperature with $T_c=121.10$ K. The C_{mag} is deduced through the correction of lattice and electronic contributions. For the first run, B^+ and B^- were 0.20 and 1.24 J K^{-1} mol^{-1}, respectively. The straight lines are drawn with the mentioned values of α and α'.

Using T_c, α, α', A^+, A^-, B^+ and B^- as seven parameters of a least-squares means, each run was fitted to the above equations. One example of this analysis is given in Fig. 4. A fairly good agreement between the experiment and calculation could be seen over the reduced temperature range of $10^{-3}<|\varepsilon_c|<10^{-1}$. Three independent scans show the identical results. Two critical indices as well as T_c are summarized as follows;

$T_c=121.13\pm0.07$ K, $\alpha=0.44\pm0.06$ and $\alpha'=0.66\pm0.03$.

3.4 Neutron scattering above T_c

We briefly summarize the theoretical aspects of the neutron magnetic scattering which are relevant to our measurements.[13] The differential cross section for the scattering of unpolarized neutrons from an initial state $\boldsymbol{k}_i$ to a final state $\boldsymbol{k}_f$, with momentum transfer $\hbar\boldsymbol{Q}=\hbar(\boldsymbol{k}_i-\boldsymbol{k}_f)$ and energy loss $\hbar\omega=\hbar^2(k_i^2-k_f^2)/2m_n$, by a system of N localized spins on a Bravais lattice is customarily written in the form;

$$\frac{d^2\sigma}{d\Omega\, d\omega}=\hbar\left(\frac{\gamma e^2}{m_e c^2}\right)^2\frac{k_f}{k_i}|f(\boldsymbol{Q})|^2\sum_\alpha(1-\hat{Q}_\alpha^2)S^\alpha(\boldsymbol{Q},\omega), \tag{7}$$

where $f(\boldsymbol{Q})$ is the atomic magnetic form factor and $S(\boldsymbol{Q},\omega)$, the so-called scattering law, is the spatial and temporal Fourier transform of the spin correlation function; i.e.,

$$S^\alpha(\boldsymbol{Q},\omega)=\frac{N}{2\pi\hbar}\sum_{\boldsymbol{R}}\int_{-\infty}^{\infty}\exp\left(i[\boldsymbol{Q}\cdot\boldsymbol{R}-\omega t]\right)\langle S_0^\alpha(0)S_{\boldsymbol{R}}^\alpha(t)\rangle\, dt. \tag{8}$$

The $S_{\boldsymbol{R}}^\alpha(t)$ is one cartesian component of the spin operator at site $\boldsymbol{R}$ and time t. Above T_c, where the spontaneous magnetization is zero and no distinction can be made among crystal orientations, the term $(1-\hat{Q}_\alpha^2)$ must be avaraged to 2/3 and all components of $S(\boldsymbol{Q},\omega)$ contribute equally to the scattering.

Through the application of linear response theory, $S(\boldsymbol{Q},\omega)$ is described in terms of a spectral weight function, $F(\boldsymbol{Q},\omega)$, and a wave-vector-dependent susceptibility, $\chi(\boldsymbol{Q})$,

$$S(\boldsymbol{Q},\omega)=S_{\text{Bragg}}(\boldsymbol{Q},\omega=0)+\frac{NS(S+1)}{3\hbar}\frac{\hbar\omega/k_BT}{1-\exp(-\hbar\omega/k_BT)}\frac{\chi(\boldsymbol{Q})}{\chi_0}F(\boldsymbol{Q},\omega), \tag{9}$$

where $\chi_0=(g\mu_B)^2S(S+1)/3k_BT$ is the susceptibility for an isolated ion and $F(\boldsymbol{Q},\omega)$ is normalized

$$\int_{-\infty}^{\infty}F(\boldsymbol{Q},\omega)\, d\omega=1. \tag{10}$$

The first term in (9) is proportional to the square of magnetization and arises from the magnetic Bragg scattering. The second term gives diffuse scattering from spin fluctuations which becomes critical scattering near T_c. The $\chi(\boldsymbol{Q})$ is defined such that $\chi(\boldsymbol{Q}=\boldsymbol{0})$ is just the macroscopic isothermal susceptibility obtained by bulk measurements. By combining (7) with (9), we arrive at a convenient expression for the critical scattering above T_c,

$$\frac{d^2\sigma}{d\Omega\, d\omega}=\frac{2}{3}N\left(\frac{\gamma e^2}{m_e c^2}\right)^2\frac{k_f}{k_i}|f(\boldsymbol{Q})|^2S(S+1)\frac{\hbar\omega/k_BT}{1-\exp(-\hbar\omega/k_BT)}\frac{\chi(\boldsymbol{Q})}{\chi_0}F(\boldsymbol{Q},\omega). \tag{11}$$

An expression for $\chi(\boldsymbol{q})$ valid for small $\boldsymbol{q}=-(\boldsymbol{Q}+2\pi\boldsymbol{\tau})$ ($2\pi\boldsymbol{\tau}$ is a reciprocal lattice vector) is found to have the familiar Ornstein-Zernike form;

$$\frac{\chi(\boldsymbol{q})}{\chi_0}=\frac{A}{\kappa^2+q^2}, \tag{12}$$

where the parameter κ is an inverse correlation length. Through the integration over ω in (11),

$$\frac{d\sigma}{d\Omega}=\frac{2}{3}N\left(\frac{\gamma e^2}{m_e c^2}\right)^2|f(\boldsymbol{Q})|^2S(S+1)\frac{\chi(\boldsymbol{q})}{\chi_0}\int_{-\infty}^{\infty}\frac{k_f}{k_i}\frac{\hbar\omega/k_BT}{1-\exp(-\hbar\omega/k_BT)}F(\boldsymbol{q},\omega)\, d\omega. \tag{13}$$

As the temperature approaches to T_c, $F(\boldsymbol{q},\omega)$ behaves like a δ-function with the centre of $\omega=0$. In this case, the static approximation is attained so that

$$k_i \cong k_f \quad \text{and} \quad \hbar\omega \ll k_B T. \tag{14}$$

Then,

$$\frac{d\sigma}{d\Omega} = \frac{2}{3} N \left(\frac{\gamma e^2}{m_e c^2}\right)^2 |f(Q)|^2 S(S+1) \frac{\chi(q)}{\chi_0} \propto T\chi(q). \tag{15}$$

This $(d\sigma/d\Omega)$ corresponds to the scattering intensity measured with a triple-axis spectrometer operated in the double-axis mode. We see that it is proportional to the wave-vector-dependent susceptibility $\chi(q)$.

The magnetic critical scattering experiments were carried out on the TUNS spectrometer installed at the Tokai establishment JRR2 reactor in the JAERI. All measurements were performed with the triple-axis spectrometer in the double-axis configuration. The monochromatized neutron beam was obtained by using a pyrolytic graphite monochromator. We employed neutron energies of 55 meV ($\lambda = 1.22$ Å) and 30 meV ($\lambda = 1.65$ Å) to satisfy static approximation. The arrangement of horizontal collimations was with a customary notation [blank (60′)-20′-20′], as is shown in Fig. 5(a). Boronic masks were placed before and after the sample to reduce the background.

The sample used here was a polyhedral as-grown single crystal with the volume of $7 \times 5 \times 4$ mm^3. It was mounted inside a hollow alminum can and packed in with helium gas. The temperature was monitored with a Pt-Co resistance thermometer which was attached to the bottom of the sample can.

A magnetic reflection around the (1 1 1) reciprocal point was chosen on this study, where the magnetic scattering cross section was relatively large compared to the nuclear reflection. Because of the small magnetic anisotropy of CoS_2, it is equivalent in the reciprocal space to scan along any directions. Taking into account the anisotropy of experimental momentum resolution in the reciprocal space, the critical scattering was measured along the [2 $\bar{1}$ $\bar{1}$] direction as shown in Fig. 5(b).

The measured profiles are presented in Fig. 6. We can see the development of critical scattering as the temperature approaches to T_c. The Ornstein-Zernike form described before was employed for $\chi(q)/\chi_0$ to analyze our experimental results. It was convoluted with the instrumental resolution function, plus the background determined at $0.1T_c$. Two parameters of A and κ were obtained by the least-squares meathod for each temperature. Critical indices ν and γ are defined as

$$a_{nn}\kappa \propto \left(\frac{T-T_c}{T_c}\right)^{\nu}, \tag{16}$$

$$\frac{\chi(q=0)}{\chi_0} \propto \left(\frac{T-T_c}{T}\right)^{-\gamma} \tag{17}$$

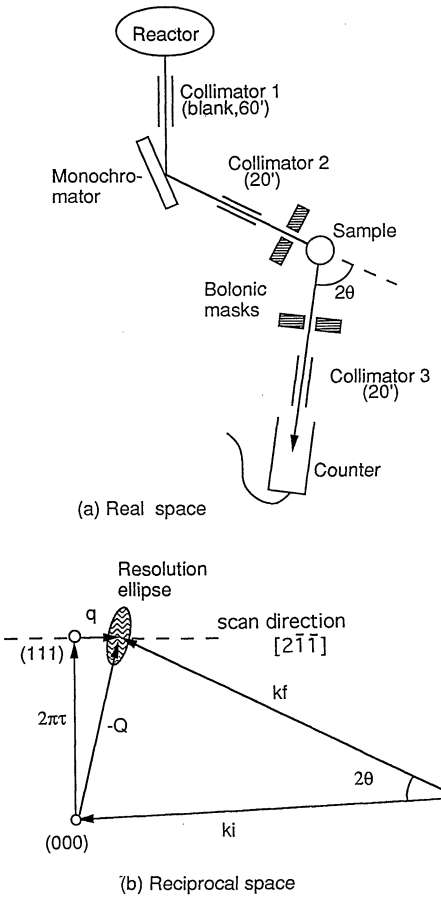

Fig. 5. Scattering diagrams in the double-axis configuration in (a) real and (b) reciproccal space.

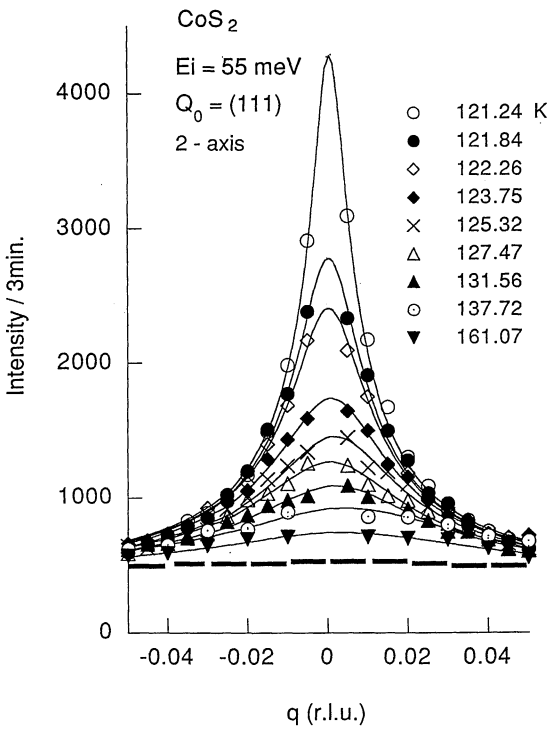

Fig. 6. Critical scattering around (1 1 1) reciprocal point at various temperaturs above T_c. Nuclear Bragg intensity of (1 1 1) is subtracted. The background is shown as a broken line.

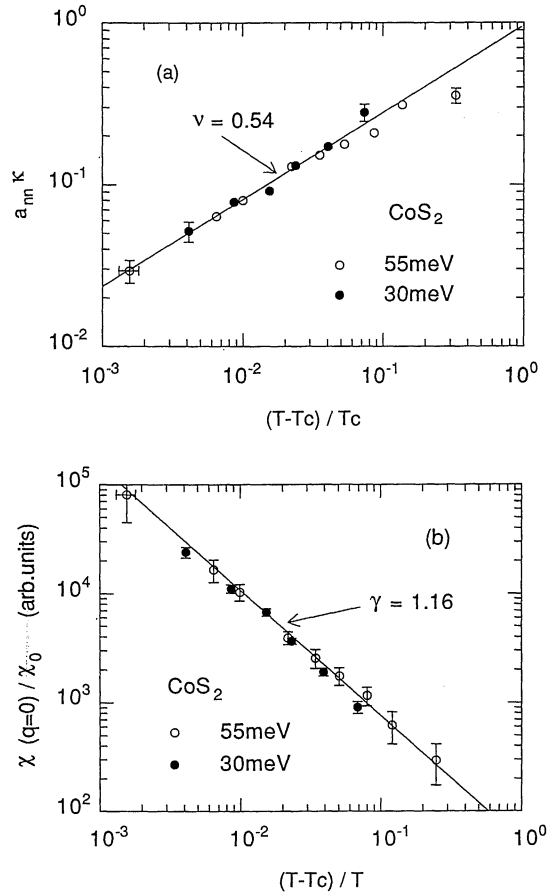

Fig. 7. Reduced temperature dependences, using $T_c=121.0$ K, of (a) the inverse spin correlation range and (b) the susceptibility of CoS_2. The straight lines are drawn with the mentioned values of ν and γ.

where a_{nn} is the nearest-neighbour distance (3.908 Å for CoS_2). The temperature dependences of both $a_{nn}\kappa$ and $\chi(q=0)/\chi_0$ are shown in log-log plots in Fig. 7. The best fits to the straight lines over the reduced temperature range between 10^{-3} and 10^{-1} resulted in $T_c=121.0\pm0.1$ K, $\gamma=1.16\pm0.10$ and $\nu=0.54\pm0.04$.

§4. Discussion and Conclusion Remarks

The experimental data of the critical indices for CoS_2 combined with the present and previous experiments are summarized in Table I together with the theoretical results for the 3*d*-Heisenberg system and those at the tricritical point. The best known experimental data of the critical indices for EuO and Ni which are either the typical insulating ferromagnet of the classical spin system or the itinerant ferromagnet are also included in the table. It must be remarked that γ values concerning the critical divergence of the magnetic susceptibility are slightly different between in the magnetization measurement and in the neutron scattering experiment, although the experimental error in the neutron scattering data is slightly bigger. One possible reason to reconcile two different values in γ is the fact that the neutron scattering is integrated over the finite frequency region by covering thermal neutrons, while the magnetization is really the static measurement at exactly $q=0$ and $\omega=0$.

Another remark in the present experiment is the fact that the specific heat measurement presented here may be more accurate than the previous measurement, and the difference in a below and above T_c is much less.

Since the anisotropy in magnetization is pretty weak in CoS_2 as shown in Fig. 1, it is

Table I. Summary of static critical indices of CoS_2 derived from the present studies (surrounded by rectangles), together with those obtained by others, other Heisenberg ferromagnets and theoretical predictions.

Index	Experiments					Theory	
	CoS_2						
	Bulk magnetization	Specific heat	Neutron scattering	EuO	Ni	3*d*-Heisenberg [k]	Tricritical [l] index
β	0.23±0.02 0.25±0.01 [a] 0.25±0.02 [b]		0.24±0.02 [d]	0.36±0.01 [e] 0.368±0.005 [f]	0.390±0.004 [h] 0.378±0.004 [i]	0.3645±0.0025	0.25
γ	1.25±0.05 1.28±0.07 [a] 1.35±0.05 [b]		1.16±0.10	1.387±0.036 [e] 1.29±0.01 [f]	1.32±0.02 [h] 1.34±0.01 [i]	1.386±0.004	1.0
δ	6.4±0.2 6.4±0.3 [a] 6.4±0.3 [b]			4.46±0.1 [f]	4.58±0.05 [i]	4.802	5.0
α		0.44±0.06 0.8±0.2 [c]		−0.09±0.01 [g]	−0.10±0.03 [j]	−0.115±0.009	0.5
α'		0.66±0.03 0.3±0.1 [c]		−0.09±0.01 [g]	−0.10±0.03 [j]	−0.115	0.5
ν			0.54±0.04	0.681±0.017 [e]	—	0.705±0.003	0.5

[a] Ref. 14. [g] Ref. 19.
[b] Ref. 15. [h] Ref. 20.
[c] Ref. 7. [i] Ref. 21.
[d] Ref. 16. [j] Ref. 22.
[e] Ref. 17. [k] Ref. 23. δ and α' are estimated from scaling laws $\delta=(\beta+\gamma)/\beta$ and $\alpha'=\alpha$, respectively.
[f] Ref. 18. [l] Ref. 9. α' is from scaling law $\alpha'=\alpha$.

quite proper to test the observed critical indices based on the 3*d*-Heisenberg ferromagnetic model. However the experimental values of CoS_2 are far different from the estimate for the 3*d*-Heisenberg ferromagnet, which gives a good fit to the EuO data. The difference between the theoretical calculation and the experimental values for Ni is much smaller. On the other hand, the experimental values in CoS_2 can reasonably be fitted to the critical indices for the tricritical values.

It must be very important whether the static scaling law is established. The scaling hypothesis is valid for the mean field calculation, while there is no rigorous theory on the critical phenomena for the weak itinerant ferromagnet in which the local moment is induced thermally. If we consider a picture that the temperature induced local magnetic moment plays an important role for ferromagnetic order, we may expect the break down of the scaling hypothesis. In fact the SCR theory predicts the reduction in the sharpness in the specific heat of which α is 0 in the mean field theory, although no quantitative estimation was given. The result testing the scaling hypothesis for the CoS_2 experiment is given in the Table II, which shows that this hypothesis holds except the equation in the first line. Another result showing the validity of the static scaling law is the fact that the scaling field H by $|T-T_c|^{\beta\delta}$ is well represented by the scaled magnetization M by $|T-T_c|^{\beta}$, $H/|T-T_c|^{\beta\delta}=f_{\pm}(M/|T-T_c|^{\beta})$, which is shown in Fig. 8. It tells us that we can't find a dominant effect of renormalized spin fluctuations on the ferromagnetic transition, since the observed magnetic transition is quite normal concerning the stable order parameter.

Then we look for another mechanism to interpret the specific values of the critical indices, in particular large α values. In fact these values are close to the critical indices of the tricritical point. The theoretical values in the table are the mean field estimate for the Gintzburg-Landau theory taking higher orders. Not only the large α values which are close to 0.5 of the mean field value at the tricritical

Table II. The result of testing the static scaling law with three dimensional system of $d=3$.

Scaling law	Experimental results
$\alpha=\alpha'$	$\alpha-\alpha'=-0.22\pm0.09$
$\alpha+2\beta+\gamma=2$	$\alpha+2(\beta-1)+\gamma_N=0.66\pm0.20$
	$\alpha+2(\beta-1)+\gamma_M=0.15\pm0.15$
$\alpha+\beta(1+\delta)=2$	$\alpha+\beta(1+\delta)-2=0.14\pm0.26$
$d\nu=2-\alpha$	$d\nu+\alpha-2=0.06\pm0.18$
$\beta+\gamma=\beta\delta$	$\beta(1-\delta)+\gamma_N=-0.08\pm0.24$
	$\beta(1-\delta)+\gamma_M=0.01\pm0.19$
$\gamma(\delta+1)$	$\gamma_N(\delta+1)-(2-\alpha)(\delta-1)=0.13\pm1.14$
$=(2-\alpha)(\delta-1)$	$\gamma_M(\delta+1)-(2-\alpha)(\delta-1)=0.81\pm0.75$

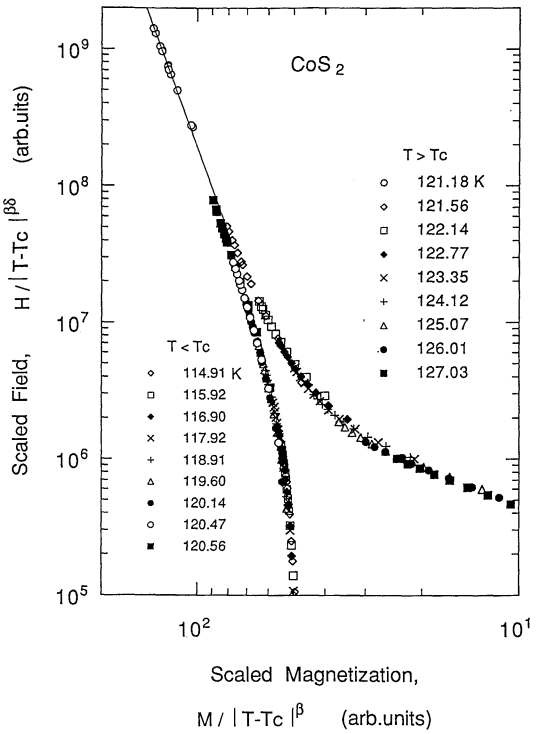

Fig. 8. Scaling law for CoS_2 with $\beta=0.23$, $\beta\delta=1.472$ and $T_c=121.13$ K. The temperature range of the data points displayed is between 4×10^{-4} and 5×10^{-2} in reduced temperature scale.

point but the fact that the experimental values hold the scaling hypothesis is favorable for the scenario that the ferromagnetic transition in CoS_2 is continuous but it is close to the tricritical point. The present scenario is most likely due to the fact that the substitution of Se to S makes the transition discontinuous. Another fact to support is the pressure dependence on the transition. Under the external pressure the temperature derivative of the magnetization near T_c becomes small,[24] which indicates larger β than the ambient β. So far the good example of the tricritical phenomena is the order-disorder transition of $[NH_4]^+$ orientation in NH_4Cl crystal.[25] The α' values for NH_4Cl and ND_4Cl are 0.57 ± 0.07 and 0.50 ± 0.07 respectively, which are close to the present result for CoS_2. Although further experiments either with $Co(Se_xS_{1-x})_2$ or under the applied pressure for CoS_2 are necessary, this new consideration that the ferromagnetic transition of CoS_2 is near the tricritical point does not include any inconsistency. If it is correct, CoS_2 provides the first real Heisenberg ferromagnet to show tricritical transition. There are several real systems showing the tricritical behavior such as $CsCoCl_3\cdot2D_2O$[26] and $FeCl_2$[27] which are all the canted magnets.

Finally we do not exclude the possibility of the existence of the temperature-induced local moment from the present experiment but we argue that the ferromagnetic transition is not influenced by the induced moment. The effect of the induced moment which is renormalized through spin fluctuations, must be dynamical in particular lower energy part. It is very important to investigate the dynamical behavior in CoS_2 not only in the critical region but in the paramagnetic region up to 400 K. We consider such scans to study on spin dynamics.

Acknowledgement

Authors thank Professor M. Collins for his suggestion of tricriticality and Professor K. Yamada for his useful discussions. They also thank M. Onodera for his technical assistance in the single crystal growth and K. Nemoto for his assistance in neutron scattering experiment. The work has been supported under the Grant in Aid for the Scientific Research by the Ministry of Education, Science and Culture, the Asahi Glass Foundation and the Research Fund of the Promotion of Science by Science Technology Agency.

References

1) H. S. Jarrett, W. H. Cloud, R. J. Bouchard, S. R. Butler, C. G. Frederick and J. L. Gillson: Phys. Rev. Lett. **21** (1968) 617.

2) K. Adachi, K. Sato and M. Takeda: J. Phys. Soc. Jpn. **26** (1969) 631.
3) K. Adachi, K. Sato, M. Okimori, G. Yamauchi, H. Yasuoka and Y. Nakamura: J. Phys. Soc. Jpn. **38** (1975) 81.
4) T. Sekiguchi, T. Miyadai and K. Manabe: J. Magn. Magn. Mater. **28** (1982) 154.
5) See, for example, *Spin Fluctuations in Itinerant Electron Magnetism*, ed. T. Moriya (Springer-Verlag, Berlin, 1985) p. 152.
6) K. Makoshi and T. Moriya: J. Phys. Soc. Jpn. **38** (1975) 10.
7) S. Ogawa and T. Yamadaya: Phys. Lett. **47A** (1974) 213.
8) K. Adachi, M. Matsui and M. Kawai: J. Phys. Soc. Jpn. **46** (1979) 1474.
9) See, for example, A. Aharony: *Critical Phenomena* (Springer-Verlag, Berlin, 1982) p. 209.
10) R. J. Bouchrd: J. Cryst. Growth **2** (1968) 40.
11) L. P. Kadanof, W. Götze, D. Hamblen, R. Hecht, E. A. S. Lewis, V. V. Palciauskas, M. Rayl and J. Swift: Rev. Mod. Phys. **39** (1967) 395.
12) A. Arrott and J. E. Noakes: Phys. Rev. Lett. **14** (1967) 786.
13) W. Marshall and S. W. Lovesey: *Theory of Thermal Neutron Scattering* (Oxford U. P., London, 1971) p. 467.
14) M. Jibu, Y. Ishikawa and K. Tajima: Phys. Lett. **45A** (1973) 235.
15) K. Adachi and K. Ohkohchi: J. Phys. Soc. Jpn. **49** (1980) 154.
16) M. Iizumi, J. W. Lynn, A. Ohsawa and H. Ito: AIP Conf. Proc. **29** (1976) 266.
17) Als-Nielsen, O. W. Dietrich and L. Passell: Phys. Rev. B **14** (1976) 4908.
18) N. Menyuk, K. Dwight and T. Reed: Phys. Rev. B **3** (1971) 1689.
19) M. B. Salamon: Solid State Commun. **13** (1973) 1741.
20) Stüser N., Rekveldt M. Th. and Spruijt T.: J. Magn. Magn. Mater. **54–57** (1986) 723.
21) Kouvel J. S., Kouvel J. B. and Comly J. B.: Phys. Rev. Lett. **20** (1968) 1237.
22) D. L. Connelly, J. S. Loomin and D. E. Mapother: Phys. Rev. B **3** (1971) 924.
23) J. C. Le Guillou and J. Zinn-Justin: Phys. Rev. **B21** (1980) 3976.
24) K. Adachi, K. Sato and M. Takeda: J. Phys. Soc. Jpn. **26** (1969) 639.
25) C. W. Garland and J. D. Baloga: Phys. Rev. B **16** (1977) 331.
26) A. L. M. Bongaarts and W. J. M. de Jonge: Phys. Rev. B **15** (1977) 3424.
27) R. J. Birgeneau, G. Shirane, M. Blume and W. C. Koehler: Phys. Rev. Lett. **33** (1974) 1098.